Emília Maria Gomes Aguiar

Implicações Ósseas na Sepse Sistêmica Aguda: Uma análise química e estrutural

Acute Systemic Sepsis Bone Implications: A chemical and structural analysis

Dissertação apresentada à Faculdade de Odontologia da Universidade de Uberlândia, para a obtenção do Título de Mestre em Odontologia na Área de Clínica Odontológica Integrada.

Uberlândia, 2018

Emília Maria Gomes Aguiar

Implicações Ósseas na Sepse Sistêmica Aguda: Uma análise química e estrutural

Acute Systemic Sepsis Bone Implications: A chemical and structural analysis

Dissertação apresentada à Faculdade de Odontologia da Universidade Federal de Uberlândia, para a obtenção do Título de Mestre em Odontologia, Área de Clínica Odontológica Integrada.

Orientador: Prof. Dr. Robinson Sabino-Silva

Banca Examinadora:
Prof. Dr. Robinson Sabino-Silva
Prof. Dra. Priscilla Barbosa Ferreira Soares
Prof. Dra. Roberta Okamoto

Uberlândia, 2018

Dados Internacionais de Catalogação na Publicação (CIP)
Sistema de Bibliotecas da UFU, MG, Brasil.

A282i
2018

Aguiar, Emília Maria Gomes, 1993
Implicações ósseas na sepse sistêmica aguda: uma análise química e estrutural / Emília Maria Gomes Aguiar. - 2018.
45 p. : il.

Orientador: Robinson Sabino da Silva.
Dissertação (mestrado) - Universidade Federal de Uberlândia, Programa de Pós-Graduação em Odontologia.
Disponível em: http://dx.doi.org/10.14393/ufu.di.2018.702
Inclui bibliografia.

1. Odontologia - Teses. 2. Osteoclastos - Teses. 3. Biomecânica - Teses. 4. Ossos - Doenças - Teses. I. Silva, Robinson Sabino da. II. Universidade Federal de Uberlândia. Programa de Pós-Graduação em Odontologia. III. Título.

CDU: 616.314

Angela Aparecida Vicentini Tzi Tziboy – CRB-6/947

SERVIÇO PÚBLICO FEDERAL
MINISTÉRIO DA EDUCAÇÃO
UNIVERSIDADE FEDERAL DE UBERLÂNDIA
FACULDADE DE ODONTOLOGIA
PROGRAMA DE PÓS-GRADUAÇÃO EM ODONTOLOGIA

Ata da defesa de DISSERTAÇÃO DE MESTRADO junto ao Programa de Pós-graduação em Odontologia, Faculdade de Odontologia da Universidade Federal de Uberlândia.

Defesa de: Dissertação de Mestrado Acadêmico **nº337**– COPOD
Data: 27/02/2018
Discente: Emília Maria Gomes Aguiar Matrícula: 11612ODO009
Título do Trabalho: ***Implicações ósseas na sepse sistêmica aguda: uma análise química e estrutural***
Área de concentração: Clínica Odontológica Integrada.
Linha de pesquisa: Processo de reparo

As **nove** horas do dia **vinte e sete de fevereiro do ano de 2018** no Anfiteatro do Bloco 4L, Campus Umuarama da Universidade Federal de Uberlândia, reuniu-se a Banca Examinadora, designada pelo Colegiado do Programa de Pós-graduação em janeiro 2018 , assim composta: Professores Doutores: Priscilla Barbosa Ferreira Soares (UFU); Roberta Okamoto (USP); e Robinson Sabino da Silva (UFU) orientador(a) do(a) candidato(a) **Emília Maria Gomes Aguiar.** Ressalta-se que o Prof. Dra. Roberta Okamoto participou da defesa por meio de Videoconferência na cidade de Araçatuba-SP e os demais membros da banca e o aluno(a) participaram *in loco*.

Iniciando os trabalhos o(a) presidente da mesa Dr. Robinson Sabino da Silva apresentou a Comissão Examinadora e o candidato(a), agradeceu a presença do público, e concedeu ao Discente a palavra para a exposição do seu trabalho. A duração da apresentação do Discente e o tempo de argüição e resposta foram conforme as normas do Programa.

A seguir o senhor (a) presidente concedeu a palavra, pela ordem sucessivamente, aos (às) examinadores (as), que passaram a argüir o (a) candidato (a). Após a argüição, que se desenvolveu dentro dos termos regimentais, a Banca, em sessão secreta, atribuiu os conceitos finais.

Em face do resultado obtido, a Banca Examinadora considerou o (a) candidato(a) A provado(a).

Esta defesa de Dissertação de Mestrado Acadêmico é parte dos requisitos necessários à obtenção do título de Mestre. O competente diploma será expedido após cumprimento dos demais requisitos, conforme as normas do Programa, a legislação pertinente e a regulamentação interna da UFU.

Nada mais havendo a tratar foram encerrados os trabalhos às 11 horas e 40 minutos. Foi lavrada a presente ata que após lida e achada conforme foi assinada pela Banca Examinadora.

Participou por meio de Videoconferência

Profª Drª Priscilla Barbosa Ferreira Soares (UFU)

Profª Drª Roberta Okamoto (USP)

Prof. Dr. Robinson Sabino da Silva UFU
Orientador (a)

DEDICATÓRIA

Dedico esse trabalho a todos aqueles que participaram comigo durante essa jornada, em especial, minha avó Maria, que nos deixou recentemente e que mesmo sem entender o que esse caminho significava, sorria sempre com as minhas vitórias. Aos meus pais Juliano e Graça, meu irmão Mateus e meu namorado Henrique, por tornarem esse sonho possível, contribuindo sempre com todo cuidado, amor e carinho. Amo vocês.

AGRADECIMENTOS

À minha família, por me apoiar sempre e ser a base de sustentação dos meus sonhos.

Ao meu noivo Henrique, que percorreu mais essa etapa ao meu lado, fazendo com que fosse mais fácil e mais feliz.

Ao meu orientador Robinson Sabino-Silva, por dividir comigo sua experiência, contribuindo para o meu crescimento e finalização deste projeto.

À Léia Cardoso, que se tornou uma grande amiga e que esteve por traz de todo o aprendizado adquirido durante o Mestrado.

À Faculdade de Odontologia da Universidade Federal de Uberlândia, por permitir o meu desenvolvimento profissional.

À FAPEMIG, que ofereceu suporte financeiro para a concretização desse sonho.

Ao ICBIM e CPBio, que disponibilizaram sua estrutura física, para que o desenvolvimento da minha pesquisa fosse possível.

Ao Prof. Dr. Gustavo Rabelo, que apesar do pouco tempo, prestou preciosas informações para a realização deste trabalho.

A todas as pessoas que participaram e que contribuíram, de alguma forma, com o desenvolvimento deste trabalho, meus sinceros agradecimentos.

EPÍGRAFE

"Dizem que antes de um rio entrar no mar, ele treme de medo. Olha para trás, para toda a jornada que percorreu, para os cumes, as montanhas, para o longo caminho sinuoso que trilhou através de florestas e povoados, e vê à sua frente um oceano tão vasto, que entrar nele nada mais é do que desaparecer para sempre. Mas não há outra maneira. O rio não pode voltar. Ninguém pode voltar. Voltar é impossível na existência. O rio precisa de se arriscar e entrar no oceano. E somente quando ele entrar no oceano é que o medo desaparece, porque apenas então o rio saberá que não se trata de desaparecer no oceano, mas de tornar-se oceano."

Osho

SUMÁRIO

Resumo

A sepse é uma resposta inflamatória do hospedeiro à uma infecção, associada a alta mortalidade, causada por danos em múltiplos órgãos, associados a alterações na calcemia. Já se sabe que as doenças inflamatórias afetam a saúde do tecido ósseo, no entanto, o efeito da sepse sistêmica aguda no tecido ósseo ainda não está bem elucidado. O objetivo deste estudo foi investigar o efeito da sepse sistêmica aguda na atividade dos osteoclastos, nas propriedades mecânicas e estruturais do osso, na composição óssea e na rugosidade superficial da tíbia. Os animais foram aleatoriamente divididos em grupo SHAM (passaram pelo procedimento cirúrgico mas não tiveram a sepse induzida) e CLP (tiveram a sepse induzida pelo método de ligação e perfuração cecal (CLP) e vinte e quatro horas após a cirurgia, os animais foram eutanasiados e as tíbias removidas. Os dados foram analisados pelo teste paramétrico t-Student e não paramétrico de Mann-Whitney com um nível de significância de 5%. Não foram observadas diferenças significativas no conteúdo mineral da tíbia entre os ratos SHAM e CLP. A sepse induziu o aumento ($p < 0,05$) no conteúdo de amida II, amida III e colágeno, que contribuiu para reduzir ($p < 0,05$) o grau de mineralização total (relação entre total de matriz orgânica/total de matriz mineral) na tíbia de CLP em comparação com ratos SHAM. Os ratos CLP também apresentaram valores mais elevados de fenilalanina (62%, $p < 0,05$) em comparação com ratos SHAM. Além disso, a sepse levou ao aumento da expressão de osteoclastos na tíbia cortical associada à redução da rugosidade superficial da tíbia. Em conjunto, mostramos que a sepse aguda promove a redução da rugosidade nanométrica associada à atividade aumentada de osteoclastos, sugerindo potencial efeito ósseo na concentração plasmática de cálcio na sepse. Finalmente, nosso estudo desvenda novos efeitos da sepse aguda na composição óssea e sugere que os pacientes acometidos pela sepse correm risco de danos ósseos.

Palavras-chaves: Biomecânica, Osso, Sepse, Rugosidade nanométrica, Osteoclastos.

Abstract

Sepsis is a host inflammatory response to infection associated with high mortality that is caused by multiple organs damages associated with changes in calcemia. It is already known that inflammatory diseases impact on the health of the bone tissue, however, the effect of systemic sepsis on bone tissue has not yet been well elucidated. The aim of this study was to investigate the effect of sepsis on osteoclast activity, bone mechanical, bone composition and surface roughness of cortical tibia. The animals were randomly divided into SHAM (passed by the surgical procedure but did not have sepsis induced) and CLP (underwent cecal ligation and puncture procedure) and twenty-four hours after surgery, animals were anesthetized to remove tibia. Data were analyzed by non-paired student t-test and Mann-Whitney non-parametric test with a significant level of 5%. No significant differences in mineral compartments of the cortical tibia could be observed between SHAM and CLP rats. Sepsis induced ($p < 0.05$) increase in amide II, amide III and collagen, which contributes to reduce ($p < 0.05$) total mineralization degree (total mineral-to-total matrix ratio) in tibia of CLP compared with SHAM rats. CLP rats also showed higher values of phenylalanine (62%, $p < 0.05$) as compared with SHAM rats. Besides, sepsis led to increased expression of osteoclasts on cortical tibia associated with reduction in surface roughness of cortical tibia. In summary, we showed that acute sepsis promotes reduction in nanometric rugosity associated with increased osteoclasts activity, suggesting a potential bone effect in plasma calcium concentration in sepsis. Finally, our study unravels new effects of acute sepsis on bone composition and suggests that septic patients are at risk of bone damage.

Keywords: Biomechanics, Bone, Sepsis, Surface roughness, Osteoclasts.

1. Introdução e Referencial Teórico

1.1. Sepse: definição, aspectos patofisiológicos e epidemiológicos

O sistema imune inato é o responsável pela regulação e manutenção do equilíbrio das respostas inflamatórias. Quando esse equilíbrio é quebrado e a reação inflamatória se torna desregulada, a ativação do sistema imune inato se torna excessiva desencadeando a Sepse (Nguyen & Smith, 2007). A sepse é caracterizada como uma síndrome clínica resultante de uma complexa interação entre o microorganismo infectante e a resposta imunológica pró-inflamatória e pró-coagulante do hospedeiro. De acordo com esta interação, ocorre uma manifestação em diferentes estágios de gravidade, o que evolui quando as alterações homeostáticas e inflamatórias aumentam em resposta a infecção. A sepse é uma condição clínica severa que representa uma resposta do corpo a um foco de infecção podendo levar a danos em múltiplos órgãos (Zhang et al., 2016). A resposta imunológica e as características do microrganismo infectante são os principais fatores envolvidos na fisiopatologia da sepse, ocorre progreção quando o organismo não consegue controlar essa infecção. A sepse inicia-se com a presença de pelo menos um foco de infecção e inflamação sistêmica, pode evoluir para uma sepse grave quando ocorre disfunção em um órgão. Nos casos em que ocorrem hipotensão arterial associado com inflamação e infecção, a doença evolui para choque séptico (Russel, 2006).

A alta taxa de prevalência acompanhada de uma alta taxa de mortalidade e da falta de tratamentos efetivos fazem com que a sepse gere altos custos para o sistema de saúde brasileiro. Além disso, a morbidade e a presença de alterações funcionais que podem ser desencadeadas pela sepse demonstram a importância da elucidação dos processos patológicos envolvidos nessa síndrome. Um estudo epidemiológico realizado em unidades de terapia intensiva (UTI) do Brasil mostrou que em uma população de 3.128 pacientes, 16,7% foram acometidos pela Sepse e desses 46,6% foram a óbito (Silva et al., 2004). Outro estudo desenvolvido nos estados de São Paulo e Santa Catarina mostrou uma incidência de sepse de 46,9%, com mortalidade de 33,9% desses pacientes. Sabe-se que esses tipos de estudos epidemiológicos sobre a sepse ainda são escassos no Brasil (Sales Jr et al., 2006). No entanto, a real incidência e a demanda de

recursos para tratamento da sepse permanecem incertos pela precariedade de informações referentes à epidemiologia da sepse. Considerando-se uma prevalência aumentada de infecções agudas que podem levar à sepse nos países de baixa e média renda (ou seja, países em que os estudos epidemiológicos da sepse são reduzidos ou até inexistentes), qualquer estimativa derivada de países desenvolvidos pode subestimar a real incidência da sepse na América Latina (Ruiz & Castell, 2016).

A sepse, resposta sistêmica à infecção, é mediada por citocinas produzidas pelas células inflamatórias que podem estimular uma série de receptores em células do sistema imunológico e de órgãos alvo. A interleucina 1 beta (IL-1β), interleucina 6 (IL-6), interleucina 8 (IL-8) e fator de necrose tumoral-alfa (TNF-α) são eventos deflagrados precocemente neste processo (Medzhitov & Janeway, 2000; Kaisho & Akira, 2001). Estas citocinas inflamatórias estimulam a liberação de outros mediadores de resposta inflamatória que podem exacerbar e contribuir na disseminação da inflamação em outros órgãos. Entre os mediadores inflamatórios estão o ácido aracdônico (PGE2), fator ativador de plaquetas (PAF) e peptídeos vasoativos como: bradicinina, angiotensina e peptídeo intestinal vasoativo (Kaisho & Akira, 2001). Percebe-se que a ação descontrolada do sistema imunológico na detecção e eliminação de microorganismos pode ser tão maléfica quanto à presença do patógeno, considerando que a sinalização para combate e eliminação do patógeno também é evidenciada na patofisiologia da sepse (Prescott & Angus, 2018).

1.2. Modelos animais de sepse

Considerando a apresentação de microbiota variada composta de bactérias gram-negativas, gram-positivas, aeróbias e anaeróbias do próprio organismo, o modelo de sepse por ligação e perfuração cecal (CLP) é amplamente utilizado e descrito como bastante eficiente. Além disso, o modelo de CLP apresenta injúria tecidual, foco infeccioso, liberação de produtos bacterianos e progressão de infecção semelhante aos casos clínicos de sepse por peritonites causadas por perfurações colônicas e diverticulites (Kingsley & Bhat, 2016).

Apesar da evidente importância dos modelos experimentais para compreensão da fisiopatologia da sepse, existe a necessidade de grande cuidado na projeção de dados obtidos em ensaios experimentais para clínicos, tendo em vista que os modelos

existentes apresentam dificuldade em mimetizar as complexidades clínicas e a heterogenicidade dos pacientes com sepse (Dejager et al., 2011).

O modelo de CLP é classicamente reconhecido pela relativa reprodutibilidade e capacidade de controle da intensidade da infecção por meio da alteração do diâmetro e da quantidade de perfurações cecais e também pelo volume fecal extravasado na cavidade peritoneal (Hubbard et al., 2005).

1.3. Osso e sepse

O osso é um tecido conjuntivo mineralizado constituído por uma matriz inorgânica formada por fosfato de cálcio, sob a forma de cristais de hidroxiapatita, associada a uma matriz orgânica composta predominantemente por colágeno tipo I e proteínas não colágenas, que juntas formam um arcabouço para a deposição dos cristais de hidroxiapatita, garantindo rigidez e resistência óssea (Boskey et al., 2002). A matriz colágena fornece ao osso a capacidade de suportar forças de tensão, enquanto que os constituintes minerais promovem capacidade de suportar cargas compressivas. Isto indica que a composição óssea e as propriedades mecânicas desempenham um papel crucial na manutenção da integridade do esqueleto (Raghavan et al., 2012).

Macroscopicamente, o tecido ósseo pode ser classificado como cortical e trabecular. O osso cortical, que representa 80% da massa esquelética, predomina em ossos longos como tíbia e fêmur. O osso trabecular, que corresponde a cerca de 20% da massa esquelética é encontrado no esqueleto axial e no interior dos ossos longos dentro de suas extremidades expandidas (metáfises e epífises). O tecido ósseo, por meio de ossos corticais e trabeculares, é o principal território de depósito mineral em organismos vertebrados ao longo da vida (Rodan & Martin, 2000) e exerce importantes funções no organismo, como a locomoção, suporte e proteção dos tecidos moles, armazenamento de cálcio e fosfato, além de abrigar a medula óssea (Kang, 2016). O tecido ósseo consiste de uma porção celular e de uma matriz extracelular. A matriz extracelular possui componentes orgânicos e inorgânicos. O componente orgânico é formado por colágeno, proteínas não-colágenas como osteocalcina e osteonectina, lipídeos e mucopolissacarídeos. A fase inorgânica é formada principalmente por cálcio e fósforo, que são depositados como sais amorfos sobre a matriz extracelular e durante o processo de mineralização óssea, formam estruturas cristalinas similares aos cristais de

hidroxiapatita [$Ca_{10}(PO_4)_6(OH)_2$]. As moléculas de colágeno formam uma estrutura tridimensional criando espaços para acomodar esses cristais (Bolean et al., 2017).

As células ósseas representam menos de 2% do tecido ósseo. No entanto, são as responsáveis pelas duas funções metabólicas chaves do osso: remodelação óssea e manutenção dos níveis circulantes de cálcio e fósforo. Neste tecido são encontrados 3 tipos principais de células: osteoblastos, osteócitos e osteoclastos, cada qual exercendo uma função importante no processo de remodelação óssea contínua, realizada por reabsorção óssea osteoclástica e formação óssea osteoblástica (Boyle et al., 2003). Os osteoblastos são células diferenciadas a partir das células mesênquimais isoladas da medula óssea. Os osteoblastos são responsáveis por secretar a matriz orgânica do osso e pela indução do processo de mineralização (Harada & Rodan, 2003). Na fase final de remodelação, os osteoblastos podem sofrer apoptose ou se incorporarem à matriz óssea recebendo o nome de osteócito. Essa célula encontrada embebida na matriz extracelular é a responsável pela manutenção da matriz óssea, coordenando a atividade osteoblástica e osteoclástica (Walsh et al., 2006; Marie & Kassem, 2011; Bellido, 2014). Já os osteoclastos, são células multinucleadas de origem hematopoiéticas que degradam o tecido ósseo através dos processos de descalcificação ácida e dissolução proteolítica (Boyle et al., 2003).

Uma série de fatores sistêmicos e locais são responsáveis pela regulação do processo de remodelação. Atualmente, sabe-se que a interação entre proteínas localizadas nas superfícies dos osteoblastos e osteoclastos são as responsáveis pela regulação local e sistêmica do processo de remodelação óssea. Neste sentido, a inflamação, além de promover a eliminação de patógenos, pode estimular a osteoclastogênese por meio das citocinas envolvidas no processo inflamatório (Thomson et al.,1987).

Lesões ósseas induzem esse processo, que é benéfico para o reparo, desde que seja um processo agudo e bem controlado. No entanto, uma resposta inflamatória suprimida, desregulada ou crônica, pode promover a destruição deste tecido (O'Keefe & Mao 2011; Waters et al., 2000). Já se sabe que doenças inflamatórias impactam na saúde do tecido ósseo, e que mesmo processos inflamatórios sub-clínicos de baixa intensidade podem impactar na remodelação óssea promovendo um aumento no risco de fraturas (Schett et al., 2006). Os pacientes com sepse ficam expostos a uma inflamação generalizada, acidemia e hipóxia e isso pode comprometer rapidamente a função óssea (Puthucheary

et al., 2017). Os testes realizados no tecido ósseo supõem que ocorra uma supressão da osteogênese e um aumento na atividade de reabsorção óssea em doenças inflamatórias como a sepse (Yang et al., 2014). Além disso, verificou-se que o lipopolissacarídeo (LPS) mimetiza a infecção bacteriana e induz expressões elevadas de genes relacionados à diferenciação de osteoclastos e genes de inflamação (Yang et al., 2014). Em um trabalho realizado por Puthucheary et al. (2017), avaliou-se alterações nas propriedades mecânicas, estruturais e histomorfométricas em fêmur de ratos acometidos pela sepse durante 24 e 96 horas. Neste trabalho, verificou-se uma diminuição do módulo de elasticidade do colágeno em animais com sepse após 24 e 96 horas da CLP, além da diminuição das propriedades mecânicas do pescoço femoral.

Um estudo realizado por Costa et al. (2013), avaliando a regulação diferencial da atividade de osteoblastos e osteoclastos por topografia superficial de revestimento de hidroxiapatita, constatou que a ligação e a diferenciação dos osteoblastos foram maiores nas superfícies micro-ásperas do que nas superfícies com topografias mais lisas; enquanto que, a atividade dos osteoclastos foi maior em superfícies mais lisas em comparação as micro-ásperas.

Dessa forma, uma vez que, os ratos não fazem remodelação intracortical (Bentolila et al., 1998) e que a rugosidade superficial do osso interfere na atividade dos osteoblastos e osteoclastos, esperamos que ocorra uma alteração na superfície da cortical óssea. Considerando ainda que tem sido observado diminuição da saúde óssea em pacientes internados em UTI e que mais de 50% desses pacientes são acometidos pela sepse (Vincent et al., 2006; Orford et al., 2011), esperamos que a sepse sistêmica aguda pode promover alterações nas propriedades mecânicas do tecido ósseo. Embora a relação direta entre condição inflamatória e defeitos ósseos tenha sido bem caracterizada, a capacidade da sepse sistêmica aguda de modular a atividade osteoclástica, a composição óssea, sua topografia superficial e suas propriedades mecânicas ainda não estão estabelecidas na sepse. Dessa forma, esse trabalho teve como objetivo investigar os efeitos da sepse sistêmica aguda: i) na composição óssea; ii) na rugosidade superficial do osso cortical; iii) na atividade dos osteoclastos; iv) nas propriedades mecânicas e; v) na microarquitetura óssea.

2. CAPÍTULOS

ARTIGO 1 - Acute Systemic Sepsis Bone Implications: A chemical and structural analysis

Artigo a ser enviado para publicação no periódico BONE

Emília Maria Gomes Aguiar, Stephanie Wutke; Léia Cardoso-Sousa; Douglas Carvalho Caixeta; Alexandre Vieira; Paula Dechichi; Carlos José Soares, Priscilla Barbosa Ferreira Soares, Luiz Ricardo Goulart; Roberta Okamoto; Robinson Sabino-Silva.

Acute Systemic Sepsis Bone Implications: A chemical and structural analysis

Emília Maria Gomes Aguiar[1], Stephanie Wutke[1]; Léia Cardoso-Sousa[1]; Douglas Carvalho Caixeta[2]; Alexandre Vieira[1]; Paula Dechichi[3]; Carlos José Soares[4], Priscilla Barbosa Ferreira Soares[5], Luiz Ricardo Goulart[2,6]; Roberta Okamoto[7]; Robinson Sabino-Silva[1*].

[1]Department of Physiology, Institute of Biomedical Sciences, Federal University of Uberlandia, Minas Gerais, Brazil.

[2]Institute of Genetics and Biochemistry, Federal University of Uberlandia, Minas Gerais, Brazil.

[3]Department of Morphology, Institute of Biomedical Sciences, Federal University of Uberlandia, Minas Gerais, Brazil.

[4]Department of Dental Materials, School of Dentistry, Federal University of Uberlândia, Minas Gerais, Brazil.

[5]Department of Periodontology and Implantology, School of Dentistry, Federal University of Uberlândia, Minas Gerais, Brazil.

[6]Department of Medical Microbiology and Immunology, University of California Davis, California, USA.

[7]Department of Basic Sciences, School of Dentistry, São Paulo State University, São Paulo, Brazil.

*Corresponding author

E-mail: robinsonsabino@gmail.com

Abstract

Sepsis is a host inflammatory response to infection that is caused by multiple organs damages. It is already known that inflammatory diseases promote damage on bone tissue, however, the chemical and structural effects of systemic sepsis on bone has not yet been well elucidated. The aim of this study was to investigate the effect of acute systemic sepsis on osteoclast activity, bone mechanical, bone composition and surface roughness of cortical tibia. Sepsis was induced by cecal ligation and puncture surgery (CLP) and twenty-four hours after surgery, animals were anesthetized to remove tibia. No significant differences in mineral compartments of the cortical tibia could be observed between SHAM and CLP rats. Sepsis induced ($p < 0.05$) increase in amide II, amide III and collagen, which contributes to reduce ($p < 0.05$) total mineralization degree (total mineral-to-total matrix ratio) in tibia of CLP compared with SHAM rats. CLP rats also showed higher values of phenylalanine (62%, $p < 0.05$) as compared with SHAM rats. Besides, sepsis led to increased expression of osteoclasts on cortical tibia associated with reduction in surface roughness of cortical tibia. In summary, we showed that acute sepsis promotes reduction in nanometric rugosity associated with increased osteoclasts activity in sepsis. Finally, our study unravels new effects of acute sepsis on bone composition and suggests that septic patients are at risk of bone damage.

1. Introduction

Sepsis is a serious clinical condition that represents a response to an infection that may lead to multiple organ damage [1]. In severe sepsis a poor prognosis with high mortality rates is achieved when organs are affected [2; 3]. Sepsis survivors are exposed to an inflammation, acidosis and hypoxia that may rapidly compromise bone health [4]. A decrease in plasma calcium was described 24 h after intraperitoneal sepsis induction [5]; however, hypocalcemia is detected around ~20% of patients [6].

Bone is a main territory of mineral deposit in vertebrate organisms throughout the life [7]. The bone promote its functions of delivering calcium to plasma while maintaining strength [8]. Bone is a metabolically active organ that undergoes continuous remodeling by osteoclastic bone resorption and osteoblastic bone formation [9]. Osteoblast attachment and differentiation were greater on micro-rough surfaces than on smoother topographies; whereas, the activity of the osteoclast was greater on smoother surfaces [10]. Osteoclasts are specialized cells that adhere to bone matrix, then secrete acid and lytic enzymes to degrade bone in extracellular compartment [11]. Whole bone strength can be determined by intrinsic properties of bone microarchitecture [12]. Several evidences indicate that bone composition and mechanical properties plays a critical role in skeletal integrity [13]. It has been suggested that Fourier-transform infrared spectroscopy (FTIR) and Raman spectroscopy can indicate changes in bone composition, which are predictors of changes in mechanical properties [13].

Bone displays suppressed osteogenesis and enhanced bone resorption activity in inflammatory diseases such as sepsis [14]. Lipopolysaccharide (LPS) induces elevated expressions of osteoclast differentiation-related genes and inflammation genes at an early stage in bone [14]. In an experimental sepsis model, trabecular femoral strength and collagen elastic modulus were reduced at 24 hours and 96 hours [4]. Although the direct relationship between inflammatory condition and bone defects was well characterized, the capacity of acute sepsis to modulate bone composition, surface topography and bone mechanical were not considered in sepsis.

We hypothesized that acute systemic sepsis promotes changes on bone composition and development of smoother surface roughness of cortical bone promoted by cortical osteoclasts. Thus, the aim of the present study was to evaluate the effects of

acute sepsis on bone tissue by osteoclast activity, composition, roughness, biomechanical and microarchitecture.

2. Methods

2.1. Experimental design

Animal procedures were approved by the Ethics Committee for Animal Research of the Federal University of Uberlandia (Proposal #45/2015). After randomization, Cecal Ligation and Puncture (CLP) induced a sublethal polymicrobial sepsis in male Wistar rats (weighing ~260g). Under anesthesia (ketamine (90 mg/kg) and xylasine (10 mg/kg), intraperitoneally) the rats received an aseptic midline laparotomy, and the portion of cecum was exteriorized and placed outside of the abdominal cavity. The cecum was partially ligated using a 4.0 silk tie and perforated with a 22-gauge needle for nine times. The cecum was gently squeezed to extrude a small amount of feces from the perforation. After that, the portion of cecum was inserted into the abdominal cavity and the laparotomy was closed using a 4.0 silk sutures. Sham animals received the same procedure by the same operator; however, the cecum was not perforated [15]. During the experimental procedures the animals were kept in dorsal recumbence. Body temperature of animals was maintained at 37.5 ± 1.5 ºC with a heating blanket. All rats were caged and allowed free access to water and standard rodent chow diet (Nuvilab CR-1; Nuvital, Curitiba, Brazil). Sham and CLP rats were studied 24 hours after sepsis induction. A direct cardiac puncture was performed in the left ventricle to collect the whole blood of the animal. After euthanasia, tibias were dissected and removed. Rights tibia were frozen in PBS in freezer -20ºC to be used in the Mechanical Test, Micro-CT, FTIR spectroscopy, Raman spectroscopy and Atomic Force Microscopy (AFM) analysis. In contrast, those on the left side were fixed in formalin and underwent histological processing. All efforts were made to minimize animal suffering. The methods were carried out in accordance with the approved guidelines.

2.2. FTIR and RAMAN spectroscopy

FTIR and RAMAN spectroscopy are techniques used to evaluate the chemical profile of the samples. For this, the ends of tibia (between the diaphysis and the proximal epiphyses) were stored – 80 °C and macerated with a sterile mortar and pestle to obtain sample spectra. Chemical profile in bone by FTIR spectra were recorded in 4000-400 cm^{-1} region using FTIR spectrophotometer Vertex 70 (Bruker, Billerica, Massachusetts, USA) associated with a micro-attenuated total reflectance (ATR) accessory. All spectra were recorded at room temperature (23±1 °C). The crystal material unit of ATR unit was a diamond disc as internal-reflection element. The sample penetration depth ranges between 0.1 and 2 μm and depends on the wavelength, the refractive index of the ATR-crystal material and the incidence angle of the beam. The infrared beam was reflected at the interface toward the sample. The air spectrum was considered as a background in FTIR analysis. Samples spectrum were taken with 4 cm^{-1} of resolution and 32 scans were performed to each analysis. The FTIR spectra were normalized and the baselines were corrected using OPUS 6.5 software (Bruker, Billerica, Massachusetts, USA) [16]. None noise removal techniques were applied. Table 1 shows the frequencies and assignments of the vibrational modes identified on bone. Briefly, in original spectra the vibrational mode 1645 cm^{-1} is identified as υNH (Amide I) bending vibrations [17; 18; 16]. The δNH (Amide II) bending vibration is usually represented in ~1548 cm^{-1} [16; 19]. The vibrational mode 1415 cm^{-1} and ~870 cm^{-1} are identified as carbonate [20]. The vibrational modes at ~1238 and ~1201 cm^{-1} are attributed to stretching vibrations of carboxyl group υCOO (amide III) and collagen, respectively [21]. Besides, spectral areas of 1010, 598 and 555 cm^{-1} vibrational modes indicate phosphate [20]. The mineral phase is defined by the parameters of carbonate substitution (Area of 850–890 cm^{-1} band/area of phosphate band), mineralization degree (area of 900–1200 cm^{-1} phosphate band/area of amide I band (1585–1720 cm − 1), mineral cristallinity (Area of 1030 cm^{-1} subband/area of 1020 cm^{-1} subband) and total mineralization degree (total mineral ratio/total matrix ratio). The protein phase can be analyzed by collagen maturity (Area of 1660 cm^{-1} subband/area of 1690 cm^{-1} subband).

To assess chemical components changes in cortical tibia by Raman spectroscopy, specimens were lyophilized and measurement were recorded in a QE65000 Spectrometer (Ocean Optics) with a 785 nm diode laser (LASER-785-IP-LAB),

assembled with diffraction grating H#6, slit of 100 μm, and Raman shift measurements were obtained and plotted from 200 to 2.000 cm^{-1}, and resolution 4 cm^{-1}. Data were processed using SpectraSuite and ASP-QE softwares. The ~959 cm^{-1} vibrational mode is attributed to Phosphate [22]. The 1070 cm^{-1} vibrational mode is attributed to carbonate [22]. The 1242 and 1272 cm^{-1} vibrational modes indicates amide III stretch observed in several proteins [22]. The 1660 cm^{-1} vibrational mode is attributed to amide I also frequently observed proteins [22].

2.3. Biomechanical testing

Twenty-four hours before mechanical test of flexion in 3 points, the tibias were thawed at -4 °C. After that, the tibias were inserted at room temperature 1-hour before testing. The specimens were maintained wrapped in the PBS-soaked gauzes except during mechanical analysis. Each right tibia was subjected to a three-point bending test until failure, using a material testing machine (EMIC DL 2000, EMIC Equipamentos e Sistemas de Ensaio Ltda, Sao José dos Pinhais, Brazil). Each specimen was positioned horizontally on the two holding fixtures of the machine, with the tibial tuberosity facing outwards, while the upper loading fixture applied the load of 50 Kgf from lateral to medial at a loading rate of 1.0 mm/min (Figure 2. A e B). The span length between holding fixtures was 12 mm and the load was applied at the center of the lengthened area. Load and displacement data were recorded and subsequently, load vs. displacement curves were plotted. Maximum load values were derived from data force (N), energy-to-fracture (mJ) and stiffness values (N/mm) were calculated as the slope of the initial linear uploading portion of the curves. After the three-point bending test, the portion of the tibia diaphysis was sectioned with a diamond disk with constant irrigation for obtain two bone segments. The distal segment was used for Micro-CT evaluation and the proximal segment for FTIR and RAMAN spectroscopy and atomic force microscopy analysis.

2.4. Micro-CT evaluation

For assessing bone micro-architecture in the experimental groups, the distal tibial diaphysis were examined using a desktop micro-CT system, commercially available as

SkyScan 1272 (Bruker, Kontich, Belgium). During scanning, the tibia were placed in the polyethylene tube and immobilized inside the tubes by means of soft modeling clay. The scanning parameters were 15 μm pixel size, 50 kV X-ray voltage, 160 mA electric current and 0.5 mm Al filter. Subsequently, the reconstructed 3D data sets were quantified using CTAn3 automated image analysis system, Fig 3.A (Bruker, Kontich, Belgium). For this, the volume-of-interest (VOI) for cortical analyses was selected and extending totally 190 slices. Cortical architecture was assessed in the diaphysis and was characterized by bone cortical volume (Ct.V, %), bone cortical thickness (Ct.Th, mm), closed porosity (Ct.Po, %), bone surface/volume ratio (BS/BV, mm^{-1}) fractal dimension (Ct.FD, a.u.) and degree of anisotropy (Ct.DA, a.u.) according to standard procedures [23; 24].

2.5. Calcemia

The blood collected by the cardiac puncture was placed in an eppendorf (São Paulo, São Paulo, Brazil) with 10 μL of heparin. To obtain the plasma the blood samples were centrifuged at 1000 rpm for 15 minutes using a centrifuge (Waltham, Massachusetts, USA). After centrifugation, it was possible to observe the separation of the blood in 3 layers in which the plasma was the supernatant, the Leukocytes the intermediate layer and the red blood cells the pellet. Plasma calcium dosing was performed using the Calcium Liquiform kit (Labtest, Lagoa Santa, Minas Gerais, Brazil) following the manufacturer's instructions. A final solution formed was homogenized and the reading was performed on a Genesys 10S UV-Vls spectrophotometer (Waltham, Massachusetts, USA) at a wavelength of 570 nm. The absorption values obtained were recorded and the plasma calcium concentration obtained.

2.6. Immunohistochemical analysis

Left tibias were dissected and fixed in 4% buffered formalin for 24 hours and washed in running water for 24 hours. The tibias were subsequently submitted to decalcification in 2% ethylene diamine tetra acetic acid (EDTA) with changes every 3 days until their complete descaling. After decalcification, the tibias were stored in 70% alcohol followed by the processing of the samples for inclusion in paraffin with alcohol,

dehydration in increasing concentrations (70%, 85%, 95% and absolute alcohol), diaphanization in xylol, inclusion in paraffin blocks and microtomy (Leica RM2125, Wetzlar, Germany) of the 5 μm thick samples.

For immunohistochemistry the cuts were mounted on gelatinized slides and the activity of the endogenous peroxidase was inhibited with hydrogen peroxide. Next, the slides underwent the antigenic recovery step with phosphate buffer citrate (pH 6.0). Polyclonal antibody produced in goats (Santa Cruz Biotechnology) against Tartrate-Resistant Acid Phosphatase (TRAP) (SC30832) was used. A choice of this antibody was found in its need to evaluate a cellular response in the bone resorption process (TRAP). Immunohistochemical experiments were performed using immunoperoxidase as a detection method. Biotinylated secondary rabbit-produced goat anti-rabbit antibody (Pierce Biotechnology) was used, the amplifier was Avidin and Biotin (Vector Laboratories) and diaminobenzidine (Dako) as chromogen. At the end of the development with diaminobenzidine, the non-staining was performed by Harris Hematoxylin. The analysis was performed using a 20x objective Nikon (Eclipse 80i, Shinagawa, Tokyo, Japan) microscope.

2.7. Analysis by Atomic Force Microscopy (AFM)

The surface roughness of cortical tibia was analyzed with a scanning probe atomic force microscopy (AFM) (SPM-9600; Shimadzu, Tokyo, Japan). The images were recorded in tapping mode with a silicium cantilever (tip curvature radius of < 10nm, Bruker, Billerica, Massachusetts, USA) at room temperature. Randomly selected sites of samples were scanned with the scanning rate of 200 kHz and 3-dimensional images were obtained and analyzed with AFM systemic software (Gwyddion).

2.8. Statistical analysis

All values reported as Mean ± SEM. Number of animals is informed in legends. Comparisons of the means were performed by non-paired student t-test and Mann-Whitney non-parametric test (GraphPad Prism version 5.00 for Windows, GraphPad Software, San Diego, CA, USA). Values of $p < 0.005$ were considered as statistically significant.

3. Results

All rats survived to the end of the protocol. The body weight at the time of samples collection was similar in sham and CLP rats.

3.1. FITR and RAMAN spectroscopy

The infrared spectrum obtained in tibia of sham and CLP rats are represented in Figure 1. The comparison of these bones spectra showed clearly changes between sham and CLP rats. The band area at 1645 cm^{-1} was identified as amide I, CLP does not change this parameter ($p > 0.05$) compared to sham rats (Figure 2A). The band area at 1548 cm^{-1} indicates amide II. This bone component was strongly increased ($p < 0.05$) in CLP than sham rats (Figure 2B). The band area at 1415 cm^{-1} determinates carbonate. This mineral component was not affected ($p > 0.05$) by CLP compared with sham rats (Figure 2C). Amide III is identified in the band area at 1238 cm^{-1}. This band area was increased ($p < 0.05$) in tibia of CLP compared with sham rats (Figure 2D). Collagen is identified in the band area at 1201 cm^{-1}. This band area was increased ($p < 0.05$) in tibia of CLP compared with sham rats (Figure 2E).The bands at 1010 cm^{-1}, 870 cm^{-1}, 598 cm^{-1} and 555 cm^{-1} are identified as phosphate, carbonate, phosphate and phosphate, respectively. Both mineral bone components were unchanged ($p > 0.05$) in CLP compared with sham rats (Figure 2F-I).

Carbonate substitution, mineralization degree (phosphate-to-amide I ratio), collagen maturity, mineral crystallinity were unchanged in tibia of CLP than sham rats (Figure 3A-D). However, the total mineralization degree (total mineral-to-total matrix ratio) was reduced ($p < 0.05$) in tibia of CLP compared with sham rats (Figure 3E).

The RAMAN spectrum obtained in tibia of sham and CLP rats are represented in Figure 4A. The comparison of these bones spectra showed similar components between sham and CLP rats. CLP does not change ($p > 0.05$) several phosphate components, proline, carbonate, CH2 deformation and Amide I. However, phenylalanine component

as increased ($p < 0.05$) in tibia of CLP compared with sham rats (Figure 4B).

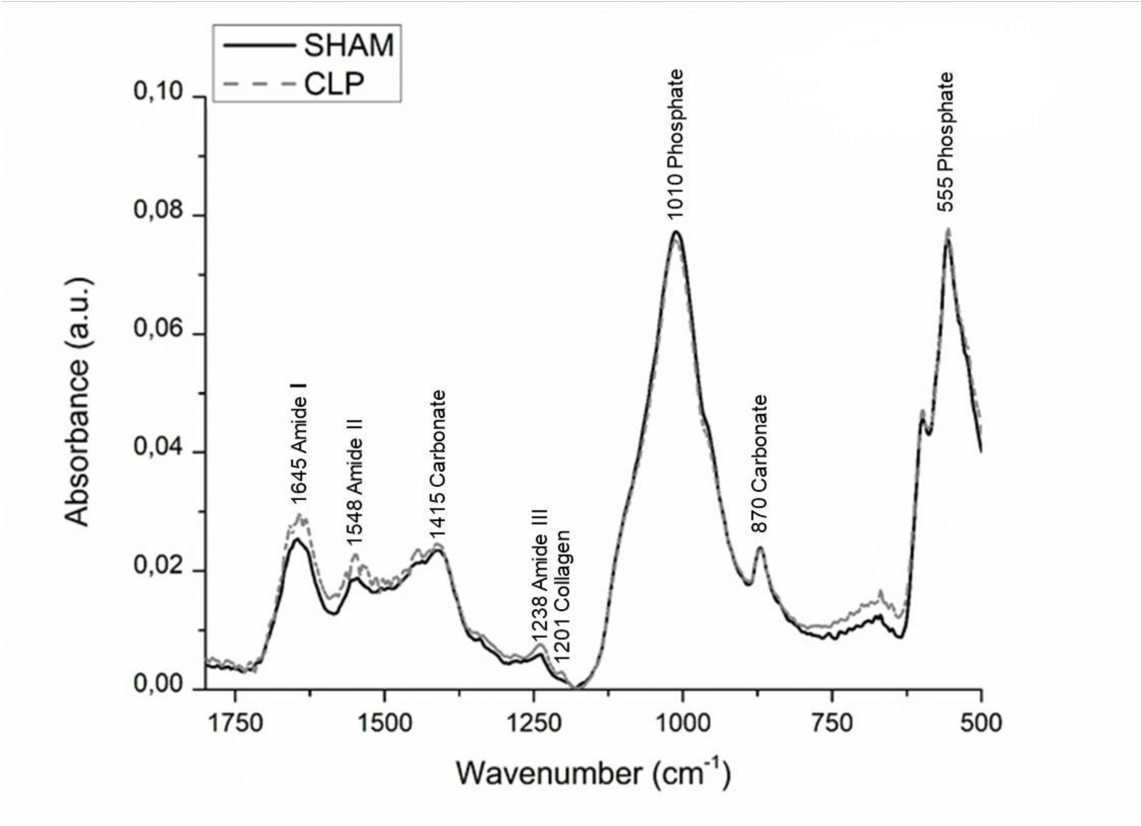

Figure 1. FTIR spectrum of bone. Mean spectrum of bone components obtained by the FTIR analysis in Sham and CLP rats.

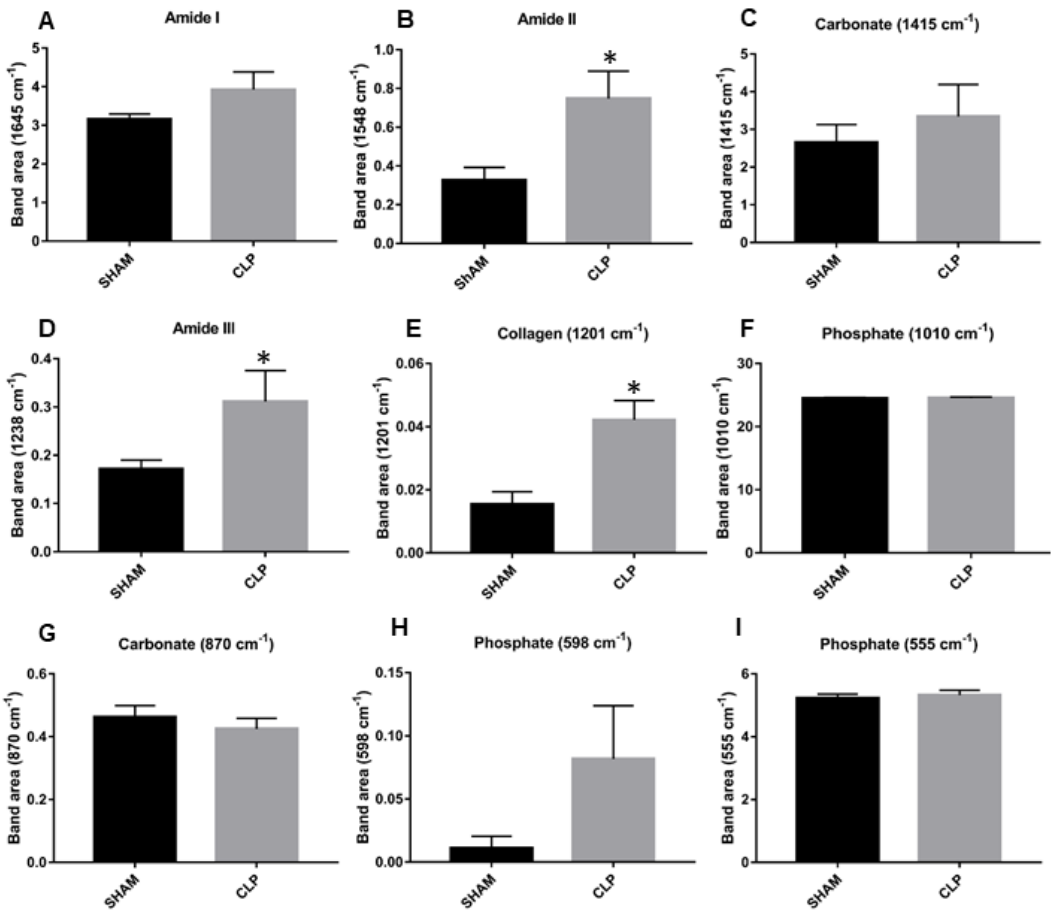

Figure 2. FTIR compositional results. Bone components evaluated in tibia of 7 SHAM and CLP rats (n = 7). **A.** Mean ± SEM of percentage of Amide I (1645 cm -1) analyzed by the non-parametric Mann-Whitney test ($p < 0.05$). **B.** Mean ± SEM of Amide II (1548 cm^{-1}) analyzed by t- Student parametric test ($p < 0.05$). **C.** Mean ± SEM of the Carbonate (1415 cm^{-1}) analyzed by t- Student parametric test ($p < 0.05$). **D.** Mean ± SEM of Amide III (1238 cm^{-1}) analyzed by the non-parametric Mann-Whitney test ($p < 0.05$). **E.** Mean ± SEM of Collagen (1201 cm^{-1}) analyzed by t- Student parametric test ($p < 0.05$). **F.** Mean ± SEM of Phosphate (1010 cm^{-1}) analyzed by t- Student parametric test ($p < 0.05$). **G.** Mean ± SEM of Carbonate (870 cm^{-1}) analyzed by t- Student parametric test ($p < 0.05$). **H.** Mean ± SEM of Phosphate (598 cm^{-1}) analyzed by the non-parametric Mann-Whitney test ($p < 0.05$) and **I.** Mean ± SEM of Phosphate (555 cm^{-1}) analyzed by t- Student parametric test ($p < 0.05$).

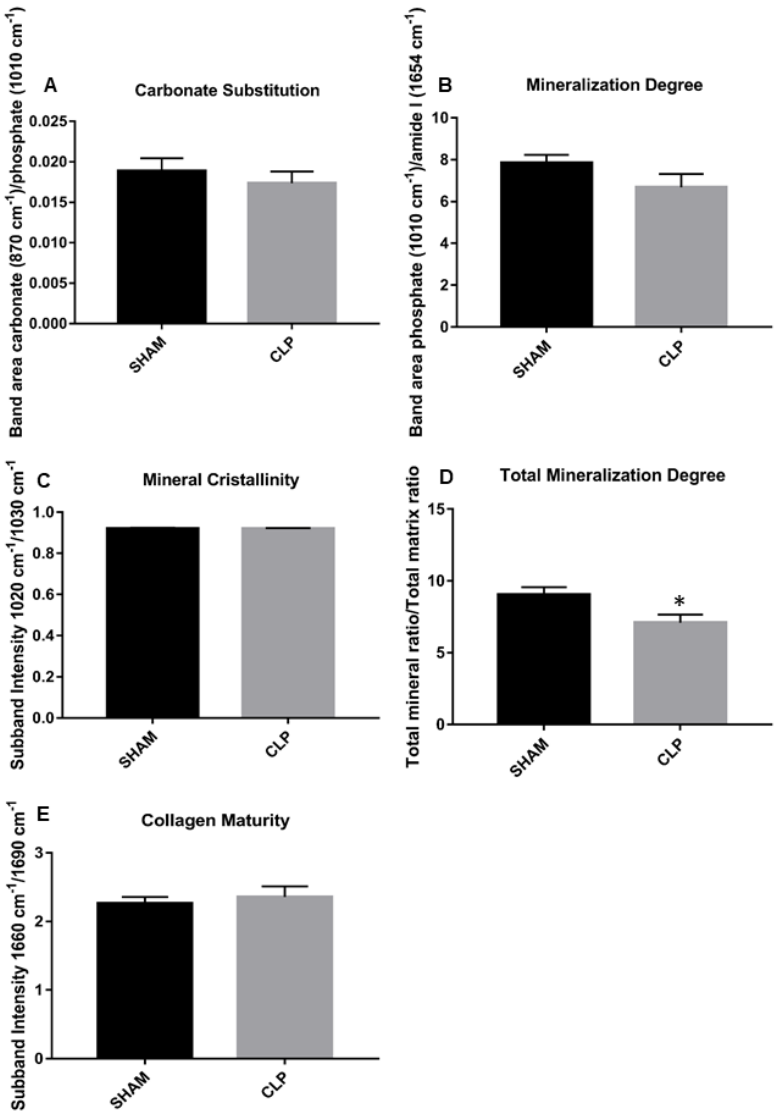

Figure 3. FTIR parameters results. Parameters evaluated in tibia of 7 SHAM and CLP rats (n = 7) and analyzed by t-Student parametric test, results are Mean ± SEM ($p < 0.05$). **A.** Carbonate Substitution. **B.** Mineralization Degree. **C.** Mineral Crystallinity. **D.** Total Mineralization Degree. **E.** Collagen Maturity.

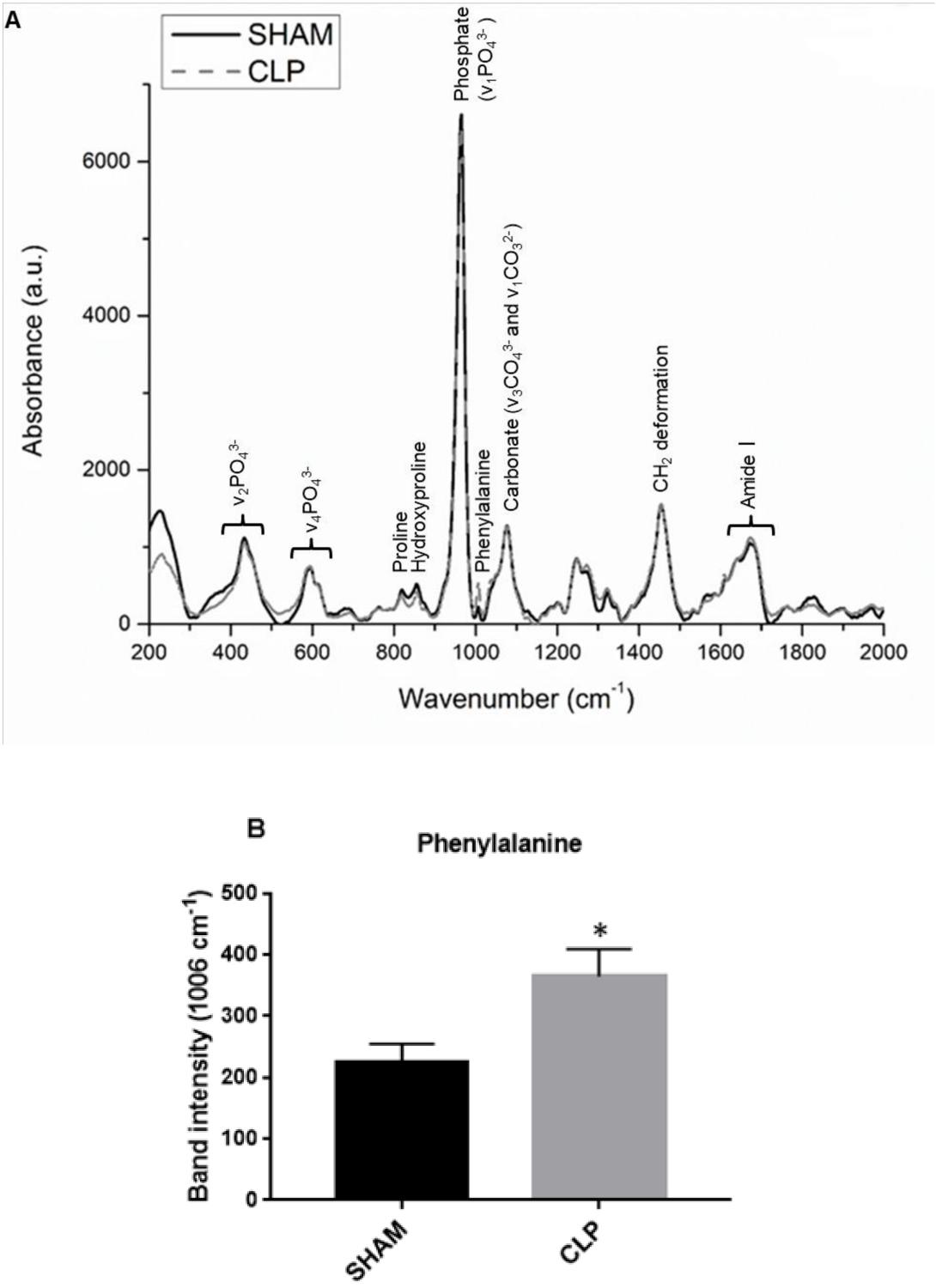

Figure 4. RAMAN spectrum and compounds. A. Mean spectrum of bone compounds obtained by the RAMAN analysis in SHAM and CLP rats. **B.** Graph of Phenylalanine with results in Mean ± SEM of 4 animals (n = 4) analyzed by t- Student parametric test ($p < 0.05$).

3.2. Biomechanical testing

The 3-point bending test produces mid-diaphysis fractures under controlled loading conditions. The primary analysis of the test measures 3 elements of biomechanical performance: force (load, or the force applied to the bone), energy to fracture (the area under the load-displacement curve) and stiffness. Sepsis had no effect ($p > 0.05$) in force, energy to fracture and stiffness than sham rats (Figure 5. A-C).

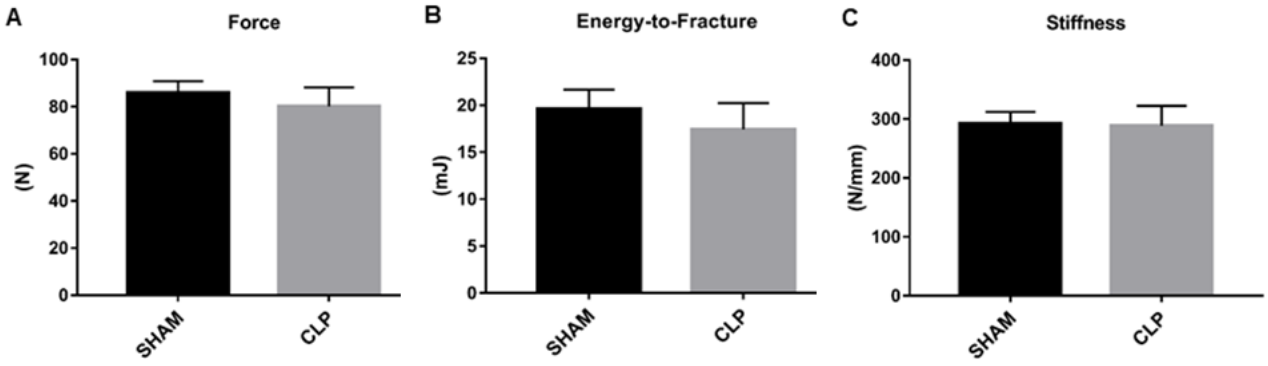

Figure 5. Biomechanical testing. Biomechanical parameters evaluated in the 3-point flexion test performed on tibiae of 7 SHAM and CLP rats ($n = 7$) and analyzed by the t-Student parametric test ($p < 0.05$). **A.** Mean ± SEM of maximum force reached until fracture (Force, N); **B.** Mean ± SEM of energy spent to fracture the bone (Energy-to-fracture, mJ); **C.** Mean ± SEM of stiffness offered by bone during force application (stiffness, N/mm).

3.3. Micro-CT evaluation

The representative 3D reconstructed micro-CT images of the cortical tibia from sham and CLP rats are shown in Figure 6 (A-B). The percent of bone volume, closed porosity, cortical thickness, fractal dimension and degree of anisotropy remained unaltered between CLP and sham rats ($p > 0.05$) (Figure 7.C-G).

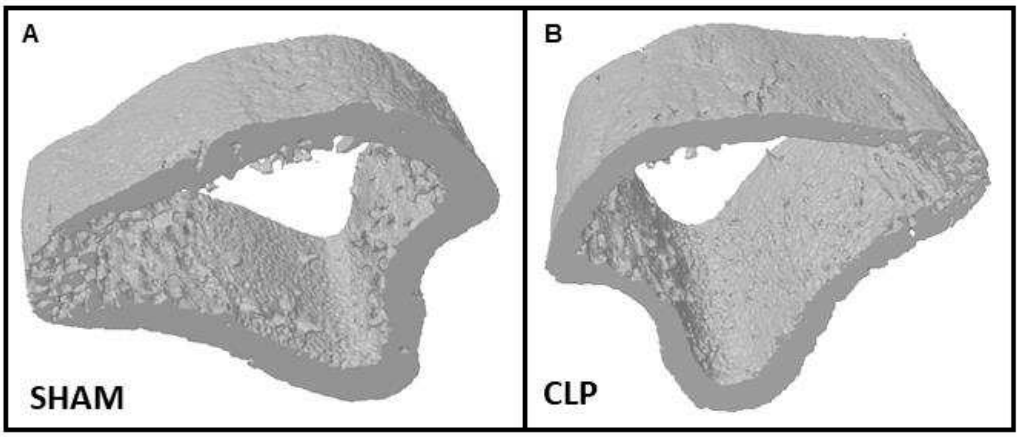

Figure 6. Micro-CT 3D rendering. Three-dimensional images of the cortical bone morphology of the rats tibia. **A.** Image of SHAM rats. **B.** Image of CLP rats.

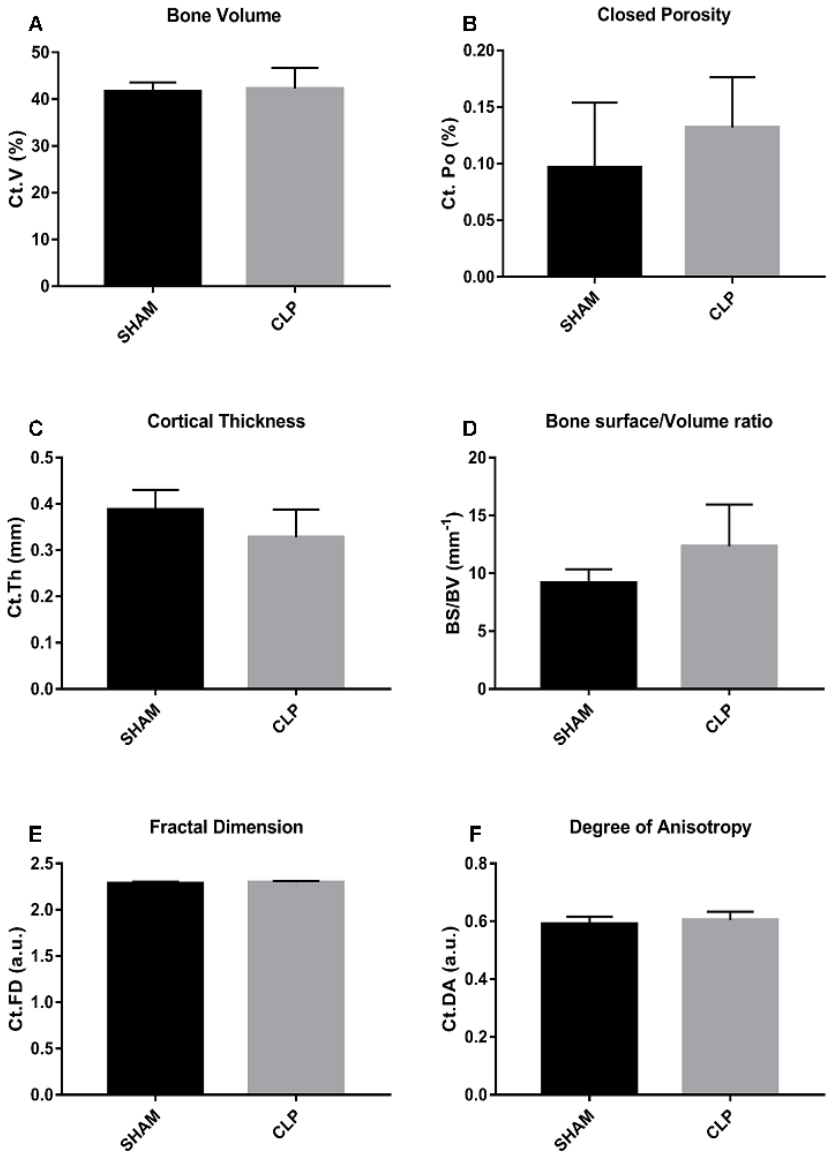

Figure 7. Micro-CT parameters. Bone Quality Parameters evaluated in the Micro-CT in tibias of 4 SHAM and CLP rats (n = 4) and analyzed by the t-Student parametric test ($p < 0.05$). **A.** Mean ± SEM of Percent of Bone Volume; **B.** Mean ± SEM of Porosity; **C.** Mean ± SEM of the Thickness of the Bone Cortical; **D.** Mean ± SEM of the Fractal Dimension; **E.** Mean ± SEM of Degree of Anisotropy.

3.4. Calcemia

To determine whether sepsis promoted changes in calcemia, calcium concentration was analyzed in plasma of CLP and sham rats. The calcemia was unchanged ($p > 0.05$) in CLP as compared with sham rats (Figure 8).

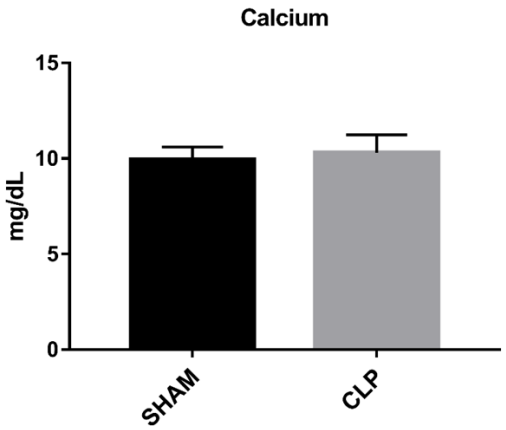

Figure 8. Calcium concentration in plasma. Mean ± SEM of the plasma calcium dosage performed in the tibia of 6 Sham and CLP rats (n = 6) animals and analyzed by t- Student' parametric test ($p < 0.05$).

3.5. Immunohistochemical analysis

Immunodetection of osteoclasts activity by TRAP is shown in Figure 8. This figure shows the TRAP Immunodetection in cortical tibiae. In parallel with presence of osteoclasts in cortical tibiae, the activity of osteoclasts by TRAP in the same territory was increased in CLP than sham rats (Figure 9A e 9B).

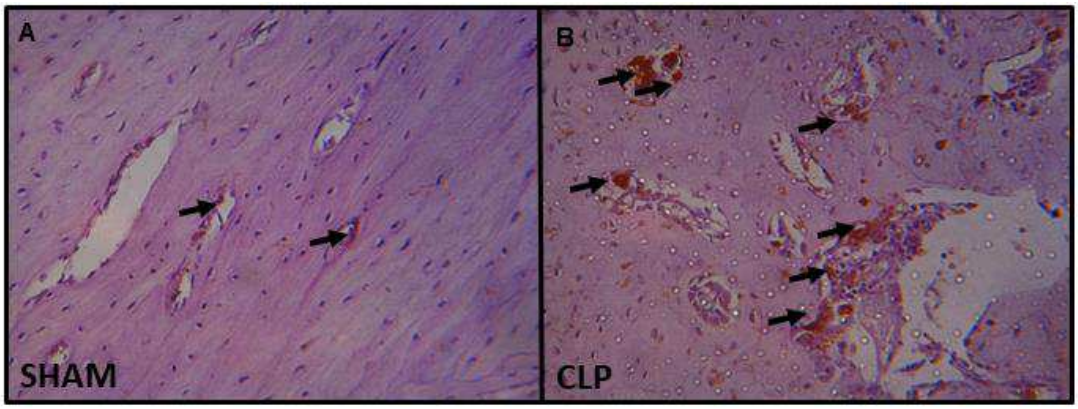

Figure 9. Tartrate-resistant acid phosphatase (TRAP) activity. Immunohistochemistry images to detect immunostaining positive for TRAP at the tibial shaft of 6 Sham and CLP rats (n = 6). **A.** Immunostaining positive for TRAP in Sham rats. **B.** Immunostaining positive for TRAP showing the increase of the osteoclast activity in CLP rats.

3.6. Analysis by Atomic Force Microscopy (AFM)

AFM measurement was implemented to examine the difference of the surface roughness of cortical bone in CLP and sham rats. As shown in Figure 10A and 10C, cortical bone of sham rats presents a nanometric roughness. On the other hand, cortical bone in CLP rats present smoother surfaces (Figure 10B and 10D).

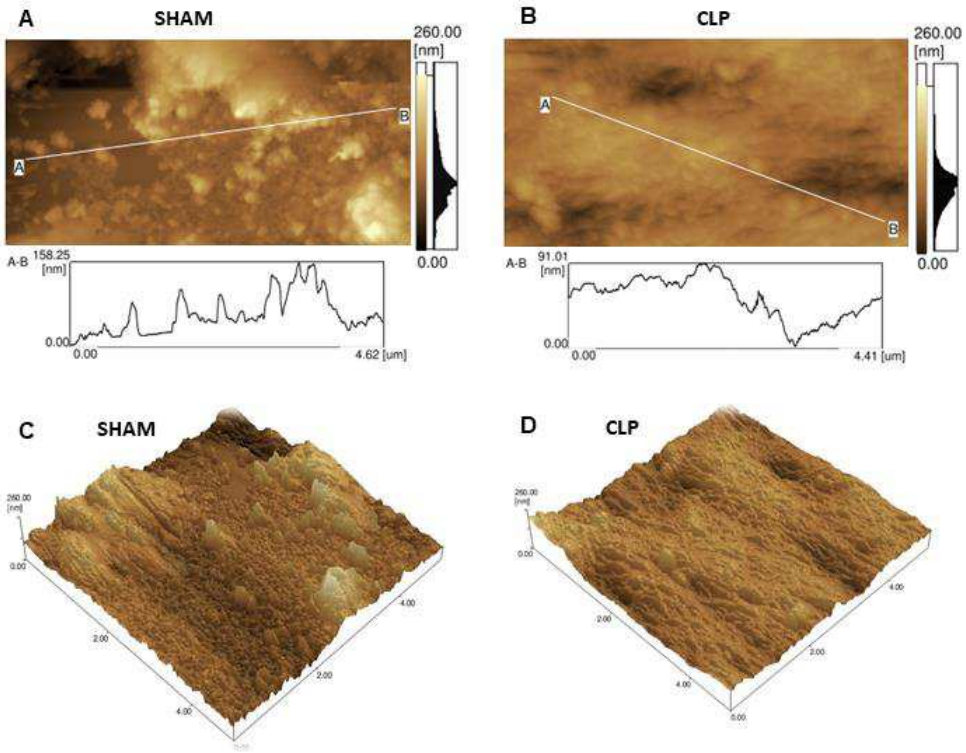

Figure 10. Bone surface roughness by Atomic force microscopy (AFM). AFM Imaging in Cortical Bone. **A and C.** Represent the surface roughness in SHAM rats. **B and D.** represent a decrease in surface roughness in CLP rats.

4. Discussion

This study clearly demonstrates that acute sepsis can promote increased osteoclasts activity on cortical tibia associated with reduction in surface roughness in this territory. Besides, Amide II, amide III and collagen were increased in tibia after acute systemic sepsis induction, indicating changes in protein composition. These changes are also accompanied by the maintenance of the bone 3-D microarchitecture and mechanical properties.

Sepsis can be induced experimentally by a procedure known as CLP, which mimic human sepsis [25; 26]. Inflammation induces bone damage by osteoblast ablation, which affects early lymphopoiesis through IL-7-mediated regulation in sepsis. Besides, it is well characterized that inflammatory-mediated osteopenia occurs via activation of osteoclast [27; 28]. Here, the functional role of cortical osteoclasts and changes in cortical bone composition were undiscovered in a classic CLP model of sepsis.

Several chronic inflammatory diseases are strongly related with bone loss [29]. Considering that almost half of patients admitted to the Intensive Care Unit are affected by sepsis [30] and bone fractures is a common endpoint in patients discharged from of intensive care unit [31], we expected change in mechanical or 3-D micro architectural properties of tibia after sepsis in rats. However, the present study indicates that acute systemic sepsis does not change force, energy to fracture and stiffness of tibial shaft. These data are in accordance with similar measurements using femoral shaft in septic rats after 24 h [5]. On the other hand, the maximum load required to fracture the femoral neck was reduced in septic rats after 24 h [5], indicating that acute systemic sepsis could promote mechanical changes in specific parts of bone. In the present study, there was no significant difference in 3-D Micro-CT reconstruction analysis in tibial shaft of septic rats, which corroborate with recently published data on bone volume/total volume ratio, trabecular thickness and separation, connectivity density, DA, and bone mineral density (BMD) in femoral neck of septic rats [5]. It is possible that this duration of mild sepsis is not sufficient to accumulate changes in mechanical or 3-D micro architectural properties detected by mechanical and micro-CT analyses, respectively. Although the present study may suggest that duration of sepsis could promote significant changes in mechanical and architectural properties, sepsis is an extremely turbulent process that brings about several temporary changes, which are not the focus of our study.

High blood phenylalanine levels and phenylketonuria are associated with bone damage [32]. Besides, a parallel relationship between plasma phenylalanine concentrations with osteoclastogenesis was described with peripheral blood mononuclear cell of patients with phenylketonuria [33]. The increase of phenylalanine content in cortical tibia by Raman spectroscopy analysis suggests a possible role of this component in enhancing osteoclastogenesis differentiation and consequently promoting bone resorption.

Cortical bone from rats with acute sepsis had greater collagen fibers, amide II and amide III content as assessed by FTIR and greater phenylalanine content as assessed by Raman spectroscopy. Bone matrix is a two-phase system composed by mineral and collagen phases. Mineral content is related in determining bone stiffness, while collagen fibers play a pivotal role in its toughness (capacity to absorb energy) [34]. TRAP is expressed by osteoclasts, it has a critical role in synthesis of type I

collagen, the main constituent of the organic matrix of bone tissue [35]. However, TRAP also produces reactive oxygen species that promote degradation of this protein. Thus, it is evident that TRAP acts on both synthesis and collagen degradation. In the present work, a positive balance was carried out in the synthesis of collagen, verified through the FTIR. Considering that reduction of collagen content can negatively affect mechanical properties of bone and increase the fracture susceptibility, the increased in collagen content may even be key molecular event for maintaining biomechanical properties of tibial shaft.

In addition, TRAP is related to the regulation of osteoblasts so that, the mineralization process occurs more quickly in situations where TRAP is not present [36]. In the present study, there was an increase in the positive immunostaining for TRAP in CLP rats, as well as an decrease in the degree of total mineralization in septic condition, which indicates a regulatory role of TRAP on mineralization process.

Amide II is a mixed C–N stretch associated with N–H in plane bend. Alterations in this component could indicate changes in protein secondary structure [37]. The higher content of Amide III in bone indicates increased in α- elastins [38], which imparts the properties of extensibility and reversible recoil, enabling tissues to withstand repetitive mechanical stress [39; 40]. The increase in protein bone composition of septic rats suggests that these alterations could prevent expected changes in mechanical properties in tibial shaft.

Osteoblast attachment and differentiation were higher on more complex, micro-rough hydroxyapatite surfaces (Ra ~2 μm) than on smoother topographies (Ra ~1 μm). In contrast, the osteoclast marker tartrate-resistant acid phosphatase activity was increased on smoother than on micro-rough surfaces [41]. Furthermore, scanning electron microscopy revealed the presence of resorption lacunae exclusively on smoother hydroxyapatite coatings [41]. Regarding that, the present study showed increased in osteoclast activity associated with reduction of nanometric roughness in cortical bone shaft of rats with experimental sepsis. It is important to highlight that the potential regulations of osteoclast activity in sepsis may contribute with regulation of calcemia, which is commonly reduced in severe sepsis. Although, the attachment of osteoclast on smoother topographies has already been described in *in vitro* studies [41];

and to the best of our knowledge, this is the first in vivo study evaluating nanometric roughness in cortical bone of animal models with experimental sepsis.

The present study could alert to the potential risk of sepsis in bone function. In summary, we showed that acute sepsis induces reduction in nanometric rugosity associated with increase in osteoclasts activity, suggesting a potential effect in plasma calcium concentration in sepsis. Finally, our study unravels new effects of acute sepsis on bone composition and suggests that septic patients are at risk of bone damage.

ADDITIONAL INFORMATION

Competing financial

The authors declare no competing financial interests.

Authors' contributions

Aguiar MGA, Wutke S, Caixeta DC, Cardoso-Sousa L and Vieira AA collected the data, conceived the research hypothesis and wrote the manuscript. Soares CJ and Soares PBF assisted with the research assays and data collection of bone mechanical and microarchitecture. Dechichi P and Okamoto R were involved in data analysis and interpretation of bone histopathological changes. Goulart LR was involved in data analysis and interpretation of raman spectroscopy. Soares CJ, Soares PBF, Dechichi P, Goulart LR and Okamoto R reviewing and editing all parts of the final document for publication. Sabino-Silva R was involved in conception and design of the study, conceived the research hypothesis and wrote the manuscript. All authors read and approved the final manuscript.

Acknowledgments

This research was supported by a grant from CAPES/CNPq (#458143/2014), FAPEMIG (#APQ-02872-16) and National Institute of Science and Technology in Theranostics and Nanobiotechnology (CNPq Process N.: 465669/2014-0). Aguiar EMG

was recipient of a FAPEMIG fellowship. We would like to thank our collaborators at the Dental Research Center in Biomechanics, Biomaterials and Cell Biology (CPbio).

References

[1] X. Zhang, N. Chang, Y. Zhang, M. Ye, et al., Bakuchiol Protects Against Acute Lung Injury in Septic Mice. Inflammation. 40 (2) (2017) 351-359, https://doi.org/10.1007/s10753-016-0481-5.

[2] L. Yicong, H. Coedy, C. Anthonya, A. Asli, et al., Sepsis-induced elevation in plasma serotonin facilitates endothelial hyperpermeability. Sci Rep. 9 (6) (2016) 22747, https://doi.org/10.1038/srep22747.

[3] H. Kang, Z. Mao, Y. Zhao, T. Yin, et al., Ethyl pyruvate protects against by regulating energy metabolism. Ther Clin Risk Manag. 12 (2016) 287-94, https://doi.org/10.2147/TCRM.S97989.

[4] Z. A. Puthucheary, Y. Sun, K. Zeng, L. H. Vu, Z. W. Zhang, R. Z. L. Lim, N. S. Y. Chew, M. E. Cove, Sepsis Reduces Bone Strength Before Morphologic Changes Are Identifiable. Crit Care Med. 45 (12) (2017) e1254-e1261. https://doi.org/10.1097/CCM.0000000000002732.

[5] A. D. Cumming, Changes in plasma calcium during septic shock. Journal of Accident & Emergency Medicine. 11 (1) (1994) 3-7.

[6] G. P. Zaloga, B. Chernow, The Multifactorial Basis for Hypocalcemia During Sepsis: Studies of the Parathyroid Hormone-Vitamin D Axis. Ann Intern Med. 107 (1) (1987) 36–41, https://doi.org/10.7326/0003-4819-107-1-36.

[7] G.A. Rodan, T.J. Martin, Therapeutic approaches to bone diseases, Science. 289 (5484) (2000) 1508-14, https://doi.org/10.1126/science.289.5484.1508.

[8] S.Harada, G.A. Rodan, Control of osteoblast function and regulation of bone mass. Nature, 423 (6937) (2003) 349, https://doi:10.1038/nature01660.

[9] W. J. Boyle, W.S. Simonet, D. L. Lacey, Osteoclast differentiation and activation. Nature. 423 (6937) (2003) 337-42, https://doi.org/10.1038/nature01658.

[10] D. O. Costa, P. D. Prowse, T. Chrones, S. M. Sims, D. W. Hamilton, A. S. Rizkalla, S. J. Dixon, The differential regulation of osteoblast and osteoclast activity by surface topography of hydroxyapatite coatings. Biomaterials. 30 (2013)7215-26, https://doi.org/10.1016/j.biomaterials.2013.06.014.

[11] W. J. Boyle, W. S. Simonet, D. L. Lacey, Osteoclast differentiation and activation. Nature. 423 (6937) (2003) 337-42.

[12] J. Wegrzyn, J. P. Roux, D. Farlay, H. Follet, R. Chapurlat, The role of bone intrinsic properties measured by infrared spectroscopy in whole lumbar vertebra mechanics: organic rather than inorganic bone matrix?. Bone. 56 (2) (2013) 229-33, https://doi.org/10.1016/j.bone.2013.06.006.

[13] M. Raghavan, N. D. Sahar, D. H. Kohn, M. D. Morris, Age-specific profiles of tissue-level composition and mechanical properties in murine cortical bone. Bone. 50 (4) (2012) 942-53, https://doi.org/10.1016/j.bone.2011.12.026.

[14] J. Yang, N. Su, X. Du, L. Chen, Gene expression patterns in bone following lipopolysaccharide stimulation. Cell Mol Biol Lett. 19 (4) (2014) 611-22, https://doi.org/10.2478/s11658-014-0216-2.

[15] M. B. Santiago, A. A. Vieira, L. L. Elias, J. A. Rodrigues, A. Giusti-Paiva, Neurohypophyseal response to fluid resuscitation with hypertonic saline during septic shock in rats. Exp Physiol. 98 (2013) 556-563, https://doi.org/10.1113/expphysiol.2012.066241.

[16] S. Khaustova, M. Shkurnikov, E. Tonevitsky, V. Artyushenko, A. Tonevitsky, Noninvasive biochemical monitoring of physiological stress by Fourier transform infrared saliva spectroscopy. Analyst. 135 (12) (2010) 3183-92, https://doi.org/10.1039/c0an00529k.

[17] M. J. Baker, J. Trevisan, P. Bassan, R. Bhargava, et al., Using Fourier transform IR spectroscopy to analyze biological materials. Nat Protoc. 9 (8) (2014) 1771-91, https://doi.org/10.1038/nprot.2014.110.

[18] N. Kourkoumelis, A. Lani, M. Tzaphlidou, Infrared spectroscopic assessment of the inflammation-mediated osteoporosis (IMO) model applied to rabbit bone. J Biol Phys. 38 (4) (2012) 623-35, https://doi.org/10.1007/s10867-012-9276-6.

[19] P. C. C. Júnior, J. F. Strixino, L. Raniero, Analysis of saliva by Fourier transform infrared spectroscopy for diagnosis of physiological stress in athletes. Research on Biomedical Engineering. 31 (2) (2015) 116-124, http://dx.doi.org/10.1590/2446-4740.0664.

[20] M. M. Figueiredo, J.A.F. Gamelas, A.G. Martins, Characterization of Bone and Bone-Based Graft Materials Using FTIR Spectroscopy, Infrared Spectroscopy. Life and

Biomedical Sciences, Prof. Theophanides Theophile (Ed.), InTech, 2012, http://dx.doi.org/10.5772/36379. Available from: https://www.intechopen.com/books/infrared-spectroscopy-life-and-biomedical-sciences/characterization-of-bone-and-bone-based-graft-materials-using-ftir-spectroscopy.

[21] L. Rieppo, S. Saarakkala, T. Närhi, H. J. Helminen, et al., Application of second derivative spectroscopy for increasing molecular specificity of Fourier transform infrared spectroscopic imaging of articular cartilage. Osteoarthritis Cartilage. 20 (5) (2012) 451-9, http://dx.doi.org/10.1016/j.joca.2012.01.010.

[22] G. S. Mandair, M. D. Morris, Contributions of Raman spectroscopy to the understanding of bone strength. Bonekey Reports. 4 (2015) 620. http://dx.doi.org/10.1038/bonekey.2014.115.

[23] G. D. Rabelo, C.Coutinho-Camillo, L. P. Kowalski, N. Portero-Muzy, J-P. Roux, P. Chavassieux, F. A. Alves, Evaluation of cortical mandibular bone in patients with oral squamous cell carcinoma. Clin Oral Invest. (2017), http://dx.doi.org/10.1007/s00784-017-2153-8.

[24] M. L. Bouxsein, S. K. Boyd, B. A. Christiansen, R. E. Guldberg, K. J. Jepsen, R. Müller, Guidelines for assessment of bone microstructure in rodents using micro–computed tomography. J Bone Miner Res, 25 (2010) 1468–1486, http://dx.doi.org/10.1002/jbmr.141.

[25] K. A. Wichterman, A. E. Baue, I. H. Chaudry, Sepsis and septic shock--a review of laboratory models and a proposal. J Surg Res. 29 (2) (1980) 189-201, http://dx.doi.org/10.1016/0022-4804(80)90037-2.

[26] J. A. Buras, B. Holzmann, M. Sitkovsky, Animal models of sepsis: setting the stage. Nat Rev Drug Discov. 4 (10) (2005) 854-65, https://doi.org/10.1038/nrd1854.

[27] A. Terashima, K. Okamoto, T. Nakashima, S. Akira, et al., Sepsis-Induced Osteoblast Ablation Causes Immunodeficiency. Immunity. 44 (6) (2016) 1434-43, https://doi.org/10.1016/j.immuni.2016.05.012.

[28] A. TerashimA, Aberrant bone remodeling during sepsis. Clin Calcium. 27 (12) (2017) 1759-1766, https://doi.org/CliCa171217591766.

[29] R. Hardy, M. S. Cooper, Bone loss in inflammatory disorders. J Endocrinol. 201 (3) (2009) 309-20, https://doi.org/10.1677/JOE-08-0568.

[30] J. L. Vincent, Y. Sakr, C.L. Sprung, V. M. Ranieri, Sepsis in European intensive care units: Results of the SOAP study*. Critical Care Medicine. 34 (2) (2006)344-353, FEB 2006, https://doi.org/10.1097/01.CCM.0000194725.48928.3A.

[31] N. R. Orford, K. Saunders, E. Merriman, M. Henry, J. Pasco, P. Stow, M. Kotowicz, Skeletal morbidity among survivors of critical illness. Crit Care Med. 39 (6) (2011) 1295-300, https://doi.org/10.1097/CCM.0b013e318211ff3d.

[32] A. B. Mendes, F. F. Martins, W. M. Cruz, L. E, da Silva, C. B. Abadesso, G. T. Boaventura, Bone development in children and adolescents with PKU. J Inherit Metab Dis. 35 (3) (2012) 425-30, https://doi.org/10.1007/s10545-011-9412-7.

[33] I. Roato, F. Porta, A. Mussa, L. D'Amico, L. Fiore, D. Garelli, M. Spada, R. Ferracini, Bone impairment in phenylketonuria is characterized by circulating osteoclast precursors and activated T cell increase. PLoS One. 5 (11) (2010) e14167, https://doi.org/10.1371/journal.pone.0014167.

[34] S. Viguet-Carrin, P. Garnero, P. D. Delmas, The role of collagen in bone strength. Osteoporos Int. 17 (3) (2006) 319-36, https://doi.org/10.1007/s00198-005-2035-9.

[35] H. C. Roberts, L. Knott, N.C. Avery, T. M. Cox, M. J. Evans, A. R. Hayman, Altered collagen in tartrate-resistant acid phosphatase (TRAP)-deficient mice: A role for TRAP in bone collagen metabolism. Calcif Tissue Int. 80 (2007) 400–410, https://doi.org/10.1007/s00223-007-9032-2.

[36] Alison. R. Hayman, Tartrate-resistant acid phosphatase (TRAP) and the osteoclast/immune cell dichotomy. Autoimmunity. 41 (3) (2008) 218-223, https://doi.org/10.1080/08916930701694667.

[37] E. P. Paschalis, R. Mendelsohn, A. L. Boskey, Infrared Assessment of Bone Quality: A Review. Clinical Orthopaedics and Related Research. 69 (8) (2011) 2170-2178, https://doi.org/10.1007/s11999-010-1751-4.

[38] M. C. Popescu, C. Vasile, O. Craciunescu, Structural analysis of some soluble elastins by means of FT-IR and 2D IR correlation spectroscopy. Biopolymers. 93 (12) (2010) 1072-84, https://doi.org/10.1002/bip.21524.

[39] L. D. Muiznieks, F. W. Keeley, Molecular assembly and mechanical properties of the extracellular matrix: A fibrous protein perspective. Biochim Biophys Acta. 1832 (7) (2013) 866-75, https://doi.org/10.1016/j.bbadis.2012.11.022.

[40] S. Rauscher, R. Pomès, Structural disorder and protein elasticity. Adv Exp Med Biol. 725 (2012) 159-83, https://doi.org/10.1007/978-1-4614-0659-4_10.
[41] D. O. Costa, P. D. Prowse, T. Chrones, S. M. Sims, D. W. Hamilton, A. S. Rizkalla, S. J. Dixon, The differential regulation of osteoblast and osteoclast activity by surface topography of hydroxyapatite coatings. Biomaterials. 34 (30) (2013) 7215-26, https://doi.org/10.1016/j.biomaterials.2013.06.014.

Referências*

Bellido T. Osteocyte-driven bone remodeling. Calcif. Tissue Int. 2014;94:25–34. https://doi.org/10.1007/s00223-013-9774-y

Bentolila V, Boyce TM, Fyhrie DP, Drumb R, Skerry TM, Schaffler MB. Intracortical remodeling in adult rat long bones after fatigue loading. Bone. 1998 Sep;23(3):275-81. https://doi.org/10.1016/S8756-3282(98)00104-5

Bolean M, Simão AMS, Barioni MB, Favarin BZ, Sebinelli HG, Veschi EA, et al. Biophysical aspects of biomineralization. Biophys Rev. 2017 Oct;9(5):747-760. https://doi.org/10.1007/s12551-017-0315-1

Boskey AL, Spevak L, Paschalis E, Doty SB, McKee MD. Osteopontin deficiency increases mineral content and mineral crystallinity in mouse bone. Calcified Tissue International. 2002;71(2):145–154. https://doi.org/10.1007/s00223-001-1121-z

Boyle WJ, Simonet WS, Lacey DL. Osteoclast differentiation and activation, Nature. 2003;423:337–342. https://doi.org/10.1038/nature01658

Costa DO, Prowse PD, Chrones T, Sims SM, Hamilton DW, Rizkalla AS, et al. The differential regulation of osteoblast and osteoclast activity by surface topography of hydroxyapatite coatings. Biomaterials. 2013;30:7215-26. https://doi.org/10.1016/j.biomaterials.2013.06.014

Dejager L, Pinheiro I, Dejonckheere E, Libert C. Cecal ligation and puncture: the gold standard model for polymicrobial sepsis? Trends Microbiol. 2011 Apr;19(4):198-208. https://doi.org/10.1016/j.tim.2011.01.001

Harada S, Rodan GA. Control of osteoblast function and regulation of bone mass. Nature. 2003;423:349–355. https://doi.org/10.1038/nature01660

Hubbard WJ, Choudhry M, Schwacha MG, Kerby JD, Rue L, Bland KI, Chaudry IH. Cecal ligation and puncture. Shock. 2005 Dec;24 Suppl 1:52-7. https://doi.org/10.1097/01.shk.0000191414.94461.7e

Kaisho T & Akira S. Dendritic-cell function in Toll-like receptor- and MyD88-knockout mice. Trends Immunol. 2001;22(2):78-83. https://doi.org/10.1016/S1471-4906(00)01811-1

Kang H, et al. Ethyl pyruvate protects against sepsis by regulating energy metabolism. Ther Clin Risk Manag. 2016; 12:287-94.

Kingsley SM & Bhat BV. Differential Paradigms in Animal Models of Sepsis. Curr Infect Dis Rep. 2016;18(9):26. https://doi.org/10.1007/s11908-016-0535-8

Marie PJ, Kassem M. Osteoblasts in osteoporosis: past, emerging, and future anabolic targets, Eur. J. Endocrinol. 2011;165:1–10. https://doi.org/10.1530/EJE-11-0132

Medzhitov R, Janeway C Jr. Innate immune recognition: mechanisms and pathways. Immunol Rev. 2000;173 (2000):89-97. https://doi.org/10.1034/j.1600-065X.2000.917309.x

Nguyen HB & Smith D. Sepsis in the 21st century: recent definitions and therapeutic advances. Am. J. Emerg. Med. 2007; 25:564–571. https://doi.org/10.1016/j.ajem.2006.08.01

O'Keefe RJ, Mao J. Bone Tissue Engineering and Regeneration: From Discovery to the Clinic—An Overview. Tissue Engineering Part B, Reviews. 2011;17(6):389-392. https://doi.org/10.1089/ten.teb.2011.0475

Orford NR, Saunders K, Merriman E, Henry M, Pasco J, Stow P, et al. Skeletal morbidity among survivors of critical illness. Crit Care Med. 2011; 39 (6):1295-300. https://doi.org/10.1097/CCM.0b013e318211ff3d

Prescott HC & Angus DC. Enhancing Recovery From Sepsis: A Review. JAMA. 2018 Jan 2;319(1):62-75. https://doi.org/10.1001/jama.2017.17687

Puthucheary ZA, Sun Y, Zeng K, Vu LH, Zhang ZW, Lim RZL, et al. Sepsis Reduces Bone Strength Before Morphologic Changes Are Identifiable. Crit Care Med. 2017;45(12):e1254-e1261. https://doi.org/10.1097/CCM.0000000000002732

Puthucheary, Y. Sun, K. Zeng, L. H. Vu, Z. W. Zhang, R. Z. L. Lim, N. S. Y. Chew, M. E. Cove, Sepsis Reduces Bone Strength Before Morphologic Changes Are Identifiable. Crit Care Med. 45 (12) (2017) e1254-e1261. https://doi.org/10.1097/CCM.0000000000002732

Raghavan M, Sahar ND, Kohn DH, Morris MD. Age-specific profiles of tissue-level composition and mechanical properties in murine cortical bone. Bone. 2012 Apr;50(4):942-53. https://doi.org/10.1016/j.bone.2011.12.026

Rodan GA, Martin TJ. Therapeutic approaches to bone diseases. Science. 2000 Sep 1;289(5484):1508-14. https://doi.org/10.1126/science.289.5484.1508

Ruiz GO & Castell CD. Epidemiology of severe infections in Latin American intensive care units. Revista Brasileira de Terapia Intensiva. 2016; 28(3):261–263.

https://doi.org/10.5935/0103-507X.20160051

Russel JA. Management of sepsis. N Engl J Med. 2006;13(355):1699-713. https://doi.org/10.1056/NEJMra043632

Sales Jr JAL, David CM, Hatum R, et al. Sepse Brasil: 11. Estudo epidemiológico da sepse em unidades de terapia intensiva brasileiras. Rev Bras Ter Intensiva. 2006; 18:9-17. https://doi.org/10.1590/S0103-507X2006000100003

Schett G, Kiechl S, Weger S, Pederiva A, Mayr A, Petrangeli M, et al. Highsensitivity C-reactive protein and risk of nontraumatic fractures in the Bruneck study. Archives of Internal Medicine. 2006; 166:2495–2501. https://doi.org/10.1001/archinte.166.22.2495

Silva E, Pedro MA, Sogayar ACB, et al. Brazilian Sepsis 10. Epidemiological Study (BASES Study). Crit Care. 2004;8: R251-R260. https://doi.org/10.1186/cc2892

Thomson BM, Mundy GR, Chambers TJ. Tumor necrosis factors alpha and beta induce osteoblastic cells to stimulate osteoclastic boné resorption. Journal of Immunology. 1987;138:775–779.

Vincent JL, Sakr Y, Sprung CL, Ranieri VM. Sepsis in European intensive care units: Results of the SOAP study*. Critical Care Medicine. 2006; 34(2):344-353. https://doi.org/10.1097/01.CCM.0000194725.48928.3A

Walsh MC, Kim N, Kadono Y, Rho J, Lee SY, Lorenzo J, et al. Osteoimmunology: interplay between the immune system and bone metabolismo. Annu. Rev. Immunol. 2006;24:33–63. https://doi.org/10.1146/annurev.immunol.24.021605.090646

Waters R V, Gamradt S C, Asnis P, Vickery B H, Avnur Z, Hill E, et al. Systemic corticosteroids inhibit bone healing in a rabbit ulnar osteotomy model. Acta Orthop Scand. 2000; 71(3):316-21. https://doi.org/10.1080/000164700317411951

Yang J, Su N, Du X, Chen L. Gene expression patterns in bone following lipopolysaccharide stimulation. Cell Mol Biol Lett. 2014 Dec;19(4):611-22. https://doi.org/10.2478/s11658-014-0216-2

Zhang X, Chang N, Zhang Y, Han Z, Li J, Zhang J. Bakuchiol Protects Against Acute Lung Injury in Septic Mice. Inflam. 2017Apr;40(2):351-359. https://doi.org/10.1007/s10753-016-0481-5

Anexos

Anexo 1: Parecer de Aprovação da Comissão de Ética na Utilização de Animais da Universidade Federal de Uberlândia.

Universidade Federal de Uberlândia
Pró-Reitoria de Pesquisa e Pós-Graduação
Comissão de Ética na Utilização de Animais (CEUA)
Rua Ceará, S/N - Bloco 2T, sala 113 – CEP 38405-315
Campus Umuarama – Uberlândia/MG – Ramal (VoIP) 3423;
e-mail:ceua@propp.ufu.br; www.comissoes.propp.ufu.br

ANÁLISE FINAL Nº 113/17 DA COMISSÃO DE ÉTICA NA UTILIZAÇÃO DE ANIMAIS PARA O PROTOCOLO REGISTRO CEUA/UFU 029/17

Projeto Pesquisa: Avaliação de parâmetros ósseos e salivares em modelos murinos de sepse experimental.

Pesquisador Responsável: Robinson Sabino da Silva

O protocolo não apresenta problemas de ética nas condutas de pesquisa com animais nos limites da redação e da metodologia apresentadas. Ao final da pesquisa deverá encaminhar para a CEUA um relatório final.

Situação: PROTOCOLO DE PESQUISA APROVADO.

OBS: A CEUA/UFU LEMBRA QUE QUALQUER MUDANÇA NO PROTOCOLO DEVE SER INFORMADA IMEDIATAMENTE AO CEUA PARA FINS DE ANALISE E APROVAÇÃO DA MESMA.